The Positive Feedback Loop of NHE1-ERK Phosphorylation Mediated by BRAF^{V600E} Mutation Contributes to Tumorigenesis and Development of Glioblastoma

Yuhui Li
Tangshan People's Hospital
Dan Li
The Cancer Institute, Tangshan People's Hospital
Yankun Liu
The Cancer Institute, Tangshan People's Hospital
Shuqing Wang
Hospital of North China University of Science and Technology
Mingyang Sun
Tangshan People's Hospital
Zhongyuan Zhang
Zunhua People's Hospital
Xuan Zheng
Nuclear Medicine Clinical Laboratory, Tangshan People's Hospital
Jingwu Li
The Cancer Institute, Tangshan People's Hospital
Yufeng Li (yufeng_li@tsrmyy.cn)
The Cancer Institute, Tangshan People's Hospital

Research Article

Keywords: glioblastoma, BRAFV600E mutation, NHE1, ERK, inhibitor

Posted Date: May 27th, 2021

DOI: https://doi.org/10.21203/rs.3.rs-523299/v1

Version of Record: A version of this preprint was published at Biochemical and Biophysical Research Communications on December 1st, 2021. See the published version at https://doi.org/10.1016/j.bbrc.2021.11.104.

Abstract

The occurrence rate of v-raf murine sarcoma viral oncogene homolog B1 (BRAF) activating mutation V600E ($BRAF^{V600E}$) in glioblastoma multiforme (GBM) is more than 50%. Na/H exchanger 1 (NHE1), a main pH regulator affecting cell microenvironment, is hyper-expressed in GBM. However, the relationship between $BRAF^{V600E}$ signal pathway and NHE1 in GMB cells remains unclear. This study found that NHE1 was a downstream target of $BRAF^{V600E}$ and an upstream factor of extracellular signal-regulated kinase (ERK). In addition, there was a positive feedback loop between NHE1-ERK phosphorylation under regulation of $BRAF^{V600E}$ mutation contributing to the proliferation and invasion of GBM cells. Moreover, the proliferation and invasion abilities of $BRAF^{V600E}$-mutant and BRAF wild type GBM cells were all suppressed by the NHE1 inhibitor, $BRAF^{V600E}$ inhibitor and combination of them. The inhibitory effect of combination of the two inhibitors was better than each single drug both in *vitro* and in *vivo*. Combination of $BRAF^{V600E}$ and NHE1 inhibitors could be considered as a new therapeutic regimen for GBM, especially for GBM with $BRAF^{V600E}$.

Introduction

Glioma accounts for about 45% of all intracranial tumors, of which more than half are glioblastoma multiforme (GBM). GBM patients often have a poor prognosis due to the invasive growth and prone to relapse after surgery of GBM[1–2]. The invasion and occurrence of GBM are complex processes with multiple factors involved.

The v-raf murine sarcoma viral oncogene homolog B1 (BRAF) is an important transduction factor of downstream mitogen activated protein kinase (MAPK) signaling pathway[3]. In gliomas, the expression level and activity of BRAF protein are positively correlated with the malignant degree of gliomas[4]. The 600th amino acid residue gene of BRAF changes from valine to glutamic acid to form continuous activated $BRAF^{V600E}$, which leads to the continuous activation of MAPK signaling pathway and changes of tumor cell proliferation and metabolism[3]. $BRAF^{V600E}$ inhibitors Vemurafenib (PLX4032) and dabrafenib (GSK21118436) have been approved for the treatment of $BRAF^{V600E}$ mutant melanoma[5]. However, studies in gliomas have shown that the inhibition of MAPK signaling pathway by $BRAF^{V600E}$ inhibitor alone is not persistent, which may be due to drug resistance or activation of compensatory mechanism[6–7]. Further search for new therapeutic targets could provide new ideas for the treatment of $BRAF^{V600E}$ mutant GBM.

Na/H exchanger 1 (NHE1) is an important transmembrane protein that regulates the intracellular pH[8]. Our research has shown that NHE1 is the main cause contributing to contraction of rat brain penetrating arteries under the condition of intracellular alkalosis caused by transient cerebral ischemia[9]. *NHE1* gene is highly expressed in malignant tumors such as breast cancer, leukemia and GBM[10–12]. Down-regulating the expression of NHE1 can inhibit the intracellular pH adjustment to inhibit breast cancer cell

metastasis[10] and induce apoptosis of leukemia cells[11]. In addition, studies have found that NHE1 protein is activated in various malignant tumor cells such as breast cancer cells, renal cancer cells and melanoma cells[13–15]. Cancer cells produce a large amount of lactic acid due to the enhancement of anaerobic glycolysis. Overexpressed and activated NHE1 can excrete H + and result in extracellular acidic microenvironment, which is conducive to the proliferation and invasion of cancer cells[16–17]. The anti-tumor effects of NHE1 inhibitors are increasingly concerned[18]: Cariporide can inhibit the proliferation and invasion of breast cancer cells[15, 19], also inhibit the proliferation of cholangiocarcinoma cells and induce apoptosis of cholangiocarcinoma cells[20]. These show that inhibition the expression and activity of NHE1 will provide a new method of tumor treatment.

In addition, KarkiP's study has shown that BRAF protein directly binds to NHE1 and enhances its activity in cervical cancer and renal cancer cells[21]. However, the regulation mechanism of NHE1 activation in GMB cells is still unknown. This study combined microenvironment regulator NHE1 and MAPK tumorigenic signaling pathway and aimed to investigate whether BRAF activates NHE1 in GBM cells and whether NHE1 mediates MAPK signaling pathway. In addition, the inhibition effects of NHE1 inhibitor alone or in combination with $BRAF^{V600E}$ inhibitor on GBM were analyzed.

Materials And Methods

Cell culture

Human glioblastoma cell lines U251 and AM38 were purchased from Saier Biotechnology Co., Ltd. (Tianjin, China). The U251 cells were cultured in DMEM/F12 medium (GIBCO BRL., Ltd., USA), the AM38 cells were cultured in RPMI 1640 medium (GIBCO BRL., Ltd., USA), supplemented with 10% fetal bovine serum (GIBCO BRL., Ltd., USA), 100 IU/ml of penicillin and 100 μg/ml of streptomycin (Beijing Dingguochangsheng Biotechnology Co., Ltd., Beijing, China). All cells were cultured at 37℃ in a humidified incubator containing 5% CO_2.

Cell proliferation assays

Cell proliferation assays were performed using MTT (Tianjin Saier Biotechnology Co., Ltd., Tianjin, China). The cells were seeded into 96-well microtiter plates (Orange Scientific, Ltd., Belgium) at a density of $1.0x10^4$ cells/well and cultured for 24 h at 37℃ in an incubator containing 5% CO_2. The cells were then respectively treated with HOE-642 (0.16 nM, CAS: 159138-80-4) or SB590885 (0.16 nM, CAS: 405554-55-4) for 24 h. Subsequently, 10 μL MTT (5 mg/mL) was added to each well. After termination of culture, the absorbance was measured at 570 nm using a microplate reader (Bio-tek, Ltd., USA). Each experiment was carried out in three replicate wells and was repeated three times.

Intracellular pH measurements

For digital imaging of cytosolic pH, cell suspensions were prepared with HEPES at the cell concentration of 4 x 10^7 cells/ml. Adding BCECF-AM/DMSO solution to the cell suspension to a final concentration of 3 μM. After incubating at 37℃ for 30 min, the cells were washed 3 times with HEPES buffer to prepare a cell suspension of 3x10^6 cells/ml. The fluorescence values of OD1 (440 nm) and OD2 (490 nm) were detected by a multifunctional microplate reader. The fluorescence ratio (FIR = OD2/OD1) reflects the pH and thus the activity of NHE1 in the cell.

Plasmids and transfection

The whole gene synthesis film $BRAF^{V600E}$ was purchased from Saier Biotechnology Co., Ltd. (Tianjin, China). The outer film and the expression vector pcDNA3.1(+) were double-digested and ligated, and positive clones were selected after transformation with XL1-blue competent E. coli (Stratagene, Co., Ltd., USA). Then, the plasmid was extracted in small amounts by alkaline lysis. After digestion and identification of the recombinant plasmid, the digested product was subjected to 0.8% agarose gel electrophoresis to identify and record the correct recombinant plasmid (5.4 kb and 2.3 kb fragment bands). All plasmids were verified by sequencing. Then, the plasmid was extracted and purified using the B-type plasmid small volume rapid extraction kit (Bodatec, Co., Ltd., Beijing, China). The U251 cells were seeded in 6-well plates and cultured for 24 h. Subsequently, the cells were respectively transfected with the pcDNA3.1(+), pcDNA3.1(+)/$BRAF^{V600E}$ using Lipofectamine 2000 Reagent (Invitrogen, Co., Ltd., USA), according to the manufacturer's protocol.

Western blot

Total protein was collected using protein lysis buffer containing 1 μl protease inhibitor (Beijing Suo Laibao Technology Co., Ltd., Beijing, China) and 1 ml radioimmunoprecipitation assay (RIPA) lysis buffer at 14,000xg for 30 min at 4℃. The total protein concentration was calculated using the BCA assay according to the kit instructions (Merck, Co., Ltd., USA). The proteins were boiled at 99℃ for 5 min. The samples were transferred to PVDF membranes (Millipore, Co., Ltd., Shanghai, China) following SDS-PAGE. Subsequently, the membranes were incubated for 1 h in blocking buffer (containing 5% skim milk), then incubated with the following primary antibodies overnight at 4℃: anti-BRAF antibody (1:1000; Rabbit. no. ab33899; Abcam, Co., Ltd., USA), anti-$BRAF^{V600E}$ antibody (1:500; Rabbit. no. ab200535; Abcam, Co., Ltd., USA), anti-NHE1 antibody (1:1000; Rabbit. no. 67363-1-Ig; abbexa, Ltd., USA), anti-Phospho-(Ser) 14-3-3 binding motif antibody (1:500; Rabbit. no. 9601S; CST, Co., Ltd., USA), anti-extracellular signal-regulated kinase (ERK) antibody (1:2000; Rabbit. no. 51068-1-AP; proteintech, Co., Ltd., USA), anti-p-ERK antibody (1:500; Rabbit. no. 9101S; CST, Co., Ltd., USA), anti-E-cadherin antibody (1:500; Rabbit. no. SRP05266; Saier Biotechnology Co., Ltd., Tianjin, China), anti-Vimentin antibody (1:500; Rabbit. no. SRP01327; Saier Biotechnology Co., Ltd., Tianjin, China), anti-RSK antibody (1:500; Rabbit. no. SRP08000; Saier Biotechnology Co., Ltd., Tianjin, China), p-RSK antibody (1:500; Rabbit. no. 9341; CST, Co., Ltd., USA), anti-GAPDH antibody (1:1000; Rabbit. no. SRP13406; Saier Biotechnology Co., Ltd., Tianjin, China). The membranes were washed 4 times in Tris-buffered saline solution with 1X TBST and incubated with horseradish peroxidase-conjugated goat-anti-rabbit antibody (Amresco Co., Ltd., USA)

for 1.5 h at RT. Following a final wash with 1X TBST, immunoreactive bands were detected using the ChampGel automatic gel imaging analyzer (Beijing SageCreation Science Co., Ltd., China). Optical band density was quantified using Image J (National Institutes of Health, Bethesda, MD, USA).

Transwell invasion assay

The cell invasion capability was detected using transwell chamber culture systems. A total of $1x10^5$ cells were placed onto a Matrigel-coated transwell chamber with serum-free opti-MEM medium (Thermo Fisher Scientific, Inc., USA). The DMEM medium containing 20% FBS was added to the lower chamber as a chemoattractant. After 24 h, the cells attached to the lower surface of the insert filter were fixed with 33% (v/v) acetic acid (glacial acetic acid: methyl alcohol = 1: 3) and stained with crystal violet and counted.

Immunoprecipitation (IP) and Western blot

IP assays and western blot were performed as described previously[35]. Briefly, the cell extracts were incubated with magnetic beads antibody complex for 5 h at 4°C. Then the complex was washed and the immunoprecipitated proteins were analyzed by SDS/PAGE, transferred onto PVDF membrane and detected using each antibody.

Animal experiment

Nude mice were obtained from Tianjin Saier Biotechnology Co., Ltd. For the subcutaneous and metastatic models, $1×10^7$/ml U251 and AM-38 cells suspended in 100 μl medium were injected subcutaneously on the left back of nude mice. SB590885 (50mg/kg) or HOE-642 (15mg/kg) were injected into the abdominal cavity per mouse every 2 days. After 3 weeks of observation, the two groups of nude mice with different tumor formation were anesthetized and photographed. All studies performed with mice were approved by the Animal Care Committee of North China University of Science and Technology. All experiments involving mice complied with local and international regulations, ethical guidelines and the ARRIVE guidelines.

Statistical analysis

All statistical analysis was performed using SPSS software version 17.0 (SPSS, Inc., Chicago, IL, USA). The data are presented as the mean ± standard deviation (SD). One-way analysis of variance was used to analyze differences between groups. Scheffe post hoc testing was used to determine pairwise differences between means. $P < 0.05$ was considered to indicate a statistically significant difference.

Results

NHE1 was activated in $BRAF^{V600E}$-mutant AM38 cells

The protein level of BRAF and $BRAF^{V600E}$ in AM38 cells were significantly higher than these in U251 cells ($P < 0.001$, $P < 0.001$) (Fig. 1A). It confirmed that AM38 cell contains $BRAF^{V600E}$-mutant. Both the

expression and phosphorylation levels of NHE1 in AM38 cells were obviously higher than those in U251 cells ($P = 0.022$, $P = 0.001$, respectively) (Fig. 1B, 1C). The FIR value of AM38 cells, which could indirectly reflect NHE1 activity, was markedly higher than that of U251 cells ($P = 0.005$) (Fig. 1D). These data suggested that the expression, phosphorylation level and activity of NHE1 might be related to $BRAF^{V600E}$ mutation.

NHE1 was a downstream factor of $BRAF^{V600E}$ and an upstream regulator of ERK

To explore the relationship between $BRAF^{V600E}$ and NHE1, the $BRAF^{V600E}$-overexpressed pcDNA3.1(+) plasmids were constructed (Fig. 2A) and the overexpression of $BRAF^{V600E}$ in U251 cells at 48 h post-transfection were confirmed ($F = 1971.738$, $P < 0.001$; pcDNA3.1(+)/$BRAF^{V600E}$ group vs pcDNA3.1(+) group $P < 0.001$) (Fig. 2B). The protein levels of $BRAF^{V600E}$ were not affected by NHE1 inhibitor HOE-642 (pcDNA3.1(+)/$BRAF^{V600E}$ group vs pcDNA3.1(+)/$BRAF^{V600E}$+HOE-642 group $P = 0.083$) (Fig. 2B). This showed that $BRAF^{V600E}$ was not affected by NHE1.

However, both NHE1 expression ($F = 29.765$, $P < 0.001$) and phosphorylated NHE1 (p-NHE1) levels ($F = 45.887$, $P < 0.001$) (Fig. 2C), as well as the FIR value (NHE1 activity) ($F = 214.093$, $P < 0.001$), in $BRAF^{V600E}$-overexpressed U251 cells were significantly upregulated compared with those of U251 cells (pcDNA3.1(+)/$BRAF^{V600E}$ group vs pcDNA3.1(+) group: $P = 0.001$, $P = 0.001$, $P = 0.001$, respectively) (Fig. 2D). HOE-642 dramatically reversed the effect of $BRAF^{V600E}$ overexpression on NHE1 activity (pcDNA3.1(+)/$BRAF^{V600E}$ group vs pcDNA3.1(+)/$BRAF^{V600E}$+HOE-642 group $P = 0.002$) (Fig. 2D), but did not affected the NHE1 expression and phosphorylation ($P = 0.961$, $P = 0.198$, respectively) (Fig. 2C). These suggested that NHE1 was a downstream factor of $BRAF^{V600E}$.

Moreover, the phosphorylated ERK (p-ERK) level was markedly increased by $BRAF^{V600E}$-overexpression, while was partially decreased by HOE-642 treatment ($F = 160.760$, $P = 0.001$; $P < 0.001$, $P < 0.001$, respectively), while total ERK levels were not affected ($F = 2.396$, $P = 0.172$) (Fig. 2E). This suggested that NHE1 inhibitor could inhibit ERK phosphorylation. These data indicated that NHE1 was involved in BRAF/ERK signal pathway as an upstream regulator of ERK.

The proliferation and invasion abilities of U251 cells enhanced by $BRAF^{V600E}$ overexpression were inversed by NHE1 inhibitor

Both the proliferation and invasion abilities of $BRAF^{V600E}$-overexpressed U251 cells were significantly enhanced compared with those of U251 at 48 h post-transfection, while the effects were significantly reversed by HOE-642 treatment (proliferation: $F = 62.197$, $P < 0.001$; $P < 0.001$, $P = 0.002$, respectively) (invasion: $F = 125.601$, $P < 0.001$; $P < 0.001$, $P < 0.001$, respectively) (Fig. 3A, 3B). In addition, the proliferation marker Ki67 and the mesenchymal cell marker Vimentin were all significantly higher in $BRAF^{V600E}$-overexpressed U251 cells, whereas epithelial cell marker E-cadherin was markedly lower, than those in U251 cells (for Ki67: $F = 277.911$, $P < 0.001$; $P < 0.001$; for Vimentin: $F = 76.854$, $P < 0.001$; $P <$

0.001; for E-cadherin: $F = 7208.162$, $P < 0.001$; $P < 0.001$) (Fig. 3C, 3D). NHE1 inhibitor HOE-642 dramatically inversed the effects of $BRAF^{V600E}$ overexpression on protein levels of Ki67 ($P = 0.001$) and Epithelial-Mesenchymal Transition (EMT) markers ($P < 0.001$, $P < 0.001$, respectively) (Fig. 3C, 3D). These data indicated that NHE1 inhibitor could repress proliferation and invasion of $BRAF^{V600E}$ GBM cells by affecting Ki67 and EMT.

The phosphorylation and activity of NHE1 were positively regulated by p-ERK

There was no significantly difference of total ribosomal S6 kinase (RSK) between U251 cells and AM38 cell ($F = 3.750$, $P = 0.060$, $P = 0.845$) (Fig. 4A left). However, the level of phosphorylated RSK (p-RSK), an active marker of ERK signal pathway, was significantly higher in AM cells than that in U251 cells ($F = 53.847$, $P = 0.060$, $P < 0.001$) (Fig. 4A right). Total ESK levels in U152 and AM38 cells were not affected by ERK agonist Honokiol and ERK inhibitor SCH772984, respectively ($P = 0.986$, $P = 0.275$) (Fig. 4A left). Whereas p-RSK was markedly increased in Honokiol-treated U251 cells compared with that in untreated U251 cells ($P = 0.001$), and was significantly decreased in SCH772984-treated AM38 cells compared with that in untreated AM38 cells ($P = 0.001$). These confirmed the effectiveness of Honokiol and SCH772984 on ERK activity.

In addition, it was found that FIR value and p-NHE1 level in Honokiol-treated U251 cells were significantly upregulated compared those in untreated U251 cells (for FIR: $F = 47.399$, $P < 0.001$; $P < 0.001$; for p-NHE1: $F = 133.299$, $P < 0.001$; $P < 0.001$), while there was no significant difference of total NH1 among indicated groups ($F = 1.384$, $P = 0.316$) (Fig. 4B, 4C). Whereas FIR value and p-NHE1 level in AM38 cells treated with SCH772984 were dramatically decreased than those in untreated AM38 cells ($P = 0.005$, $P < 0.001$, respectively) (Fig. 4B, 4C). These data suggested that NEH1 could be phosphorylated and activated by p-ERK. Co-IP analysis confirmed that NHE1 directly interacted with $BRAF^{V600E}$ in AM38 cells, but not with wild type BRAF ($BRAF^{WT}$) and ERK (Fig. 4D).

The combination of NHE1 inhibitor and $BRAF^{V600E}$ inhibitor had better inhibitory effects on proliferation and invasion abilities of GBM cells with $BRAF^{V600E}$

The NHE1 activities (FIR) in U251 were suppressed by NHE1 inhibitor HOE-642, but not by the $BRAF^{V600E}$ inhibitor SB590885 ($F = 14.950$, $P = 0.001$, HOE-642 group vs. DMSO group $P = 0.011$, SB590885 group vs. DMSO group $P = 0.892$) (Fig. 5A left). The NHE1 activities in AM38 cells were suppressed by HOE-642, SB590885, as well as combination of them, respectively ($F = 101.013$, $P < 0.001$, HOE-642 group vs. DMSO group $P < 0.001$, SB590885 group vs. DMSO group $P < 0.001$, HOE-642 + SB590885 group vs. DMSO group $P < 0.001$) (Fig. 5A right). The combination of HOE-642 and SB590885 had better inhibitory effects on NHE1 activities than HOE-642 or SB590885 alone in AM38 cells (HOE-642 + SB590885 group vs. HOE-642 group $P = 0.011$; vs SB590885 group $P = 0.030$) (Fig. 5A right).

Both the proliferation and invasion abilities of U251 cells were inhibited by HOE-642, but not by SB590885 (proliferation: $F = 12.109$, $P = 0.002$; $P = 0.037$, $P = 0.979$,Fig. 5B left; invasion: $F = 30.379$, $P <$

0.001; $P = 0.003$, $P = 0.699$, Fig. 5C left). Both the proliferation and invasion abilities of AM38 cells were suppressed by HOE-642, SB590885, as well as combination of them, respectively (proliferation: $F = 33.877$, $P < 0.001$; $P = 0.007$, $P = 0.002$, $P < 0.001$, Fig. 5B right; invasion: $F = 89.933$, $P < 0.001$; $P < 0.001$, $P < 0.001$, $P < 0.001$, Fig. 5C right). The combination of HOE-642 and SB590885 had better inhibitory effects both on proliferation and invasion of AM38 cells than HOE-642 or SB590885 alone (proliferation: HOE-642 + SB590885 group vs. HOE-642 group $P = 0.009$; vs. SB590885 group $P = 0.043$; invasion: HOE-642 + SB590885 group vs. HOE-642 group $P < 0.001$; vs. SB590885 group $P = 0.044$) (Fig. 5A right).

The Ki67 levels in U251 cells treated with HOE-642, SB590885 and combination of them were respectively suppressed by 41.5%, 47.5% and 63.0% compared with DMSO group ($F = 22.672$, $P = 0.006$; $P = 0.030$, $P = 0.019$, $P = 0.007$), while combination of HOE-642 and SB590885 has no advantage than each alone ($P = 0.208$, $P = 0.402$) (Fig. 5D left). The Ki67 levels in AM38 cells of the three groups were respectively suppressed by 28.5%, 33.1% and 55.0% compared with DMSO group ($F = 51.534$, $P = 0.001$; $P = 0.014$, $P = 0.008$, $P = 0.001$), while the inhibition effect of the combination group was better than each drug alone ($P = 0.036$) (Fig. 5D right).

For the EMT marker, the E-cadherin in U251 cells were markedly upregulated by HOE-642, but not by SB590885 ($F = 45.423$, $P = 0.002$; $P = 0.006$, $P = 0.764$, Fig. 5E left), while E-cadherin in AM38 cells were significantly increased by HOE-642, SB590885, as well as combination of them, respectively ($F = 191.572$, $P < 0.001$; $P = 0.024$, $P = 0.003$, $P < 0.001$, Fig. 5E right). On the other hand, the Vimentin in U251 cells were markedly downregulated by HOE-642, but not by SB590885 ($F = 38.388$, $P = 0.002$; $P = 0.031$, $P = 0.895$, Fig. 5F left), while those in AM38 cells were not changed by HOE-642 or SB590885 alone ($F = 28.796$, $P = 0.004$; $P = 0.266$, $P = 0.083$, Fig. 5F right). The effects of combination of HOE-642 and SB590885 on E-cadherin and Vimentin in AM38 cells were better than each single drug (E-cadherin: $P < 0.001$, $P = 0.001$, Fig. 5E right; Vimentin: $P = 0.013$, $P = 0.030$, Fig. 5F right). These data indicated that the combination of $BRAF^{V600E}$ inhibitor and NHE1 inhibitor has better inhibitory effects on proliferation and invasion abilities of GBM cells with $BRAF^{V600E}$.

The combination of $BRAF^{V600E}$ inhibitor and NHE1 inhibitor had better inhibitory effects on GBM cells with $BRAF^{V600E}$ in vivo

To further explore the inhibitory effects of combined $BRAF^{V600E}$ inhibitor and NHE1 inhibitor on GBM cells, nude mice tumorigenesis experiments were conducted. All nude mice were in good health and activity before treatment and did not die until the end of the experiment. Figure 6A shows tumor formation in nude mice in each group. There were no significantly difference of body weight among all the indicated groups (U251: $F = 0.452$, $P = 0.718$; AM38: $F = 0.293$, $P = 0.830$) (Fig. 6B). The U251 tumor volumes were markedly downregulated by HOE-642, but not by SB590885 ($F = 22.387$, $P < 0.001$; $P = 0.007$, $P = 0.954$) (Fig. 6C). The AM38 tumor volumes were significantly decreased by HOE-642, SB590885, as well as combination of them, respectively ($F = 22.823$, $P < 0.001$; $P = 0.001$, $P = 0.001$, $P < 0.001$) (Fig. 6C). The inhibitory effects of combination of HOE-642 and SB590885 on tumor volumes of U251 and AM38 cells were better than each single drug (U251: $P = 0.040$, $P < 0.001$, AM38: $P = 0.049$, $P =$

0.026, Fig. 6C). These indicated that the inhibitory effects of combination of HOE-642 and SB590885 on tumor volumes of U251cells and AM38 cells were better than each single drug.

In addition, the AM38 tumor weight was markedly higher than U251 tumor weight (Fig. 6D left, middle). The U251 tumor wrights treated with HOE-642, SB590885 and combination of them were respectively suppressed by 41.9%, 30.0% and 64.2% compared with DMSO group, respectively ($F = 30.620$, $P < 0.001$; $P < 0.001$, $P = 0.003$, $P < 0.001$) (Fig. 6D, right). The AM38 tumor weights of the three groups were respectively suppressed by 63.1%, 62.9% and 78.8% compared with DMSO group, respectively ($F = 107.482$, $P < 0.001$; $P < 0.001$, $P < 0.001$, $P < 0.001$) (Fig. 6D, right). Moreover, the inhibitory effects of combination of HOE-642 and SB590885 on tumor weights of U251 cells and AM38 cells were all better than each single drug (U251: $P = 0.033$, $P = 0.001$; AM38: $P = 0.030$, $P = 0.029$) (Fig. 6D right). These data confirmed that the combination of $BRAF^{V600E}$ inhibitor and NHE1 inhibitor has better inhibitory effects on proliferation of U251 cells than each single drug *in vivo*.

Discussion

The present study found that the expression, phosphorylation and activity of NHE1 in $BRAF^{V600E}$-mutant AM38 cells were all higher than those in $BRAF^{WT}$ U251 cells. Overexpression of $BRAF^{V600E}$ activated the ERK pathway and upregulated the expression, phosphorylation and activity of NHE1, as well as the cell viabilities, invasion abilities and corresponding markers. Those effects of $BRAF^{V600E}$ overexpression were reversed by NHE1 inhibitor HOE-642. These data indicated that NHE1 is a downstream target of $BRAF^{V600E}$ and an upstream factor of ERK. The microenvironment factor NHE1 interacts with $BRAF^{V600E}$/ERK oncogenic signaling pathway in GBM cells.

This work also found that NHE1 was directly interacted with $BRAF^{V600E}$ in $BRAF^{V600E}$ GBM cells. This is consistent with the report in malignant melanoma cells, in which stimulated NHE1 by $BRAF^{V600E}$ induced to aberrant pH[22]. There was speculated that a similar mechanism may exist in cancer cells with $BRAF^{V600E}$ mutation. Moreover, the transport activity of NHE1 regulated by multiple intracellular signaling molecules, including MAPK/ERK[23] and PI3K/AKT kinases[24–25], those interact with different site of serine residues of the cytosolic C-terminus and phosphorylate NHE1. Additionally, we found that both the phosphorylation and activity of NHE1 were positively regulated by ERK activator and inhibitor in GBM cells, but not NHE1 expression. These suggested that there is a positive feedback loop between NHE1-ERK phosphorylation under regulation of $BRAF^{V600E}$ mutation contributing to the proliferation and invasion of GBM cells (Fig. 7). However, we did not detected interaction between NHE1 and ERK in $BRAF^{V600E}$ GBM cells. We speculated that $BRAF^{V600E}$ may have the advantage structure to combine with NHE1 in compared with BRAF and ERK in GBM cells. Evidences have suggested the ERK, MEK, RSK, RAF-1, PAK5, and 14-3-3 exist as complexes in some cell types[26–31]. The interaction between NHE1 and PI3K/AKT signaling pathways in GBM cells should be considered in the further study.

In addition, the proliferation and invasion abilities of $BRAF^{V600E}$-mutant and $BRAF^{WT}$ GBM cells, as well as the corresponding markers, were all suppressed by the NHE1 inhibitor, $BRAF^{V600E}$ inhibitor and combination of them. The inhibitory effect of combination of the two inhibitors in $BRAF^{V600E}$-mutant cells was better than each single drug both in *vitro* and in *vivo*. This probably partly due to the inhibition of some compensation mechanism by the two inhibitors in $BRAF^{V600E}$-mutant GBM cells. For the persistence of suppressive effect of combination treatment, this work only observed data by day 21. Further study should be performed.

There have several selective inhibitors to be invested and used for clinical treatment of tumors with $BRAF^{V600E}$ mutation: (1) Vemurafenib (PLX4032) could selectively bind to the ATP-binding site of $BRAF^{V600E}$ and inhibits its activity[32]. A clinical case report showed that children GBM with $BRAF^{V600E}$ mutation received Vemurafenib treatment and achieved clinical complete remission (Robinson et al., 2014). (2) UAI-201 promotes GBM cell cycle inhibition and autophagy by blocking $BRAF^{V600E}$/MEK/ERK pathway in glioma cells with $BRAF^{V600E}$ [4]. (3) Dabrafenib (GSK2118436) was approved for unresectable or metastatic melanoma and anaplastic thyroid cancer harbouring the $BRAF^{V600E}$ mutation as monotherapy or in combination with trametinib (a MAPK kinase inhibitor)[5, 34]. Our work showed that SB590885 is also an effective inhibitor for GBM with $BRAF^{V600E}$ mutation in vivo and in vitro, which provides a basis for clinical application. Moreover, HOE-642 is another candidate drug for GBM cells $BRAF^{V600E}$ mutation and has good synergistic effect with $BRAF^{V600E}$ inhibitor. These data could enlighten treatment for breast cancer and cholangiocarcinoma[19, 20, 35].

To conclude, the present study clarified that microenvironment factor NHE1 involves in $BRAF^{V600E}$/ERK oncogenic signaling pathway and contributes to the proliferation and invasion of GBM cells. Combination of $BRAF^{V600E}$ and NHE1 inhibitors probably considered as a new therapeutic regimen for future research and clinical application of GBM with $BRAF^{V600E}$.

Declarations

Author Contribution

YHL and DL performed most of the experiments and wrote the manuscript. YKL and SQW guided experimental technology. MYS performed some of the experiments. ZYZ and XZ guided and performed statistical analysis. YFL and JWL conceived the project and supervised the experiments. All authors read and approved the final manuscript.

Acknowledgements

This work was supported by Science and Technology Innovation Team Training Plan Project Fund of Tangshan (18130203B), 2019 City Talent Project Fund of Tangshan (A201905007) and Fund of Key Laboratory of Hebei Province (SZX2020043).

Conflicts interest

The authors declare no competing interests.

References

1. Liu, R. Z. *et al.* Association between cytoplasmic CRABP2, altered retinoic acid signaling, and poor prognosis in glioblastoma. *Glia.* **64**, 963–976 (2016).
2. Jiang, J. *et al.* Regorafenib induces lethal autophagy arrest by stabilizing PSAT1 in glioblastoma. *Autophagy.* **16**, 106–122 (2020).
3. Davies, H. *et al.* Mutations of the BRAF gene in human cancer. *Nature.* **417**, 949–954 (2002).
4. Ahn, J. H., Lee, Y. W., Ahn, S. K. & Lee, M. Oncogenic BRAF inhibitor UAI-201 induces cell cycle arrest and autophagy in BRAF mutant glioma cells. *Life Sci.* **104**, 38–46 (2014).
5. Jang, S. & Atkins, M. B. Treatment of BRAF-mutant melanoma: The role of vemurafenib and other therapies. *Clin Pharmacol Ther.* **95**, 24–31 (2014).
6. Yao, T. W. *et al.* EGFR blockade prevents glioma escape from BRAFV600E targeted therapy. *Oncotarget.* **6**, 21993–22005 (2015).
7. Zhang, J. *et al.* Combined $BRAF^{V600E}$ and MEK blockade for $BRAF^{V600E}$-mutant gliomas. *Neurooncol*. **131**,495–505. (2017).
8. Stock, C. & Pedersen, S. F. Roles of pH and the Na+/H + Exchanger NHE1 in Cancer: From Cell Biology and Animal Models to an Emerging Translational Perspective. *Semin Cancer Biol.* **43**, 5–16 (2017).
9. Li, Y. H., Horiuchi, T., Murata, T. & Hongo, K. Mechanism of alkalosis-induced constriction of rat cerebral penetrating arterioles. *Neuroscience Research.* **70**, 98–103 (2011).
10. Chen, Q. *et al.* Increased NHE1 expression is targeted by specific inhibitor cariporide to sensitize resistant breast cancer cells to doxorubicin in vitro and in vivo. *BMC Cancer.* **19**, 211–223 (2019).
11. Rich, I. N., Worthington-White, D., Garden, O. A. & Musk, P. Apoptosis of leukemic cells accompanies reduction in intracellular pH after targeted inhibition of the Na+/H + exchanger. *Blood.* **95**, 1427–1434 (2000).
12. Guan, X. D. *et al.* Elevated Na/H Exchanger 1 (SLC9A1) Emerges as a Marker for Tumorigenesis and Prognosis in Gliomas. *J Exp Clin Cancer Res.* **37**, 255–270 (2018).
13. Ludwig, F. T., Schwab, A. & Stock, C. The Na+ /H+ -Exchanger (NHE1) Generates pH Nanodomains at Focal Adhesions. *J Cell Physiol.* **228**, 1351–1358 (2013).
14. Karumanchi, S. A. *et al.* VHL tumor suppressor regulates Cl−/HCO3− exchange and Na+/H + exchange activities in renal carcinoma cells. *Physiol Genomics.* **5**, 119–128 (2001).
15. Wang, J. *et al.* CIAPIN1 targets Na(+)/H(+) exchanger 1 to mediate MDA-MB-231 cells' metastasis through regulation of MMPs via ERK1/2 signaling pathway. *Exp Cell Res.* **333**, 60–72 (2001).

16. Neri, D. & Supuran, C. T. Interfering with pH regulation in tumors as a therapeutic strategy. *Nat Rev Drug Discov.* **10**, 767–777 (2001).
17. Brisson, L., Reshkin, S. J., Goré, J. & Roger, S. pH regulators in invadosomal functioning: proton delivery for matrix tasting. *Eur J Cell Biol.* **91**, 847–860 (2012).
18. Harguindey, S. *et al.* Cariporide and other new and powerful NHE1 inhibitors as potentially selective anticancer drugs an integral molecular/biochemical/metabolic/clinical approach after one hundred years of cancer research. *J Transl Med.* **11**, 282–298 (2013).
19. Lin, Y. N. *et al.* NHE1 mediates MDA-MB-231 cells invasion through the regulation of MT1-MMP. *Exp Cell Res.* **317**, 2031–2040 (2011).
20. Sario, A. D. *et al.* Selective inhibition of ion transport mechanisms regulating intracellular pH reduces proliferation and induces apoptosis in cholangiocarcinoma cells. *Dig Liver Dis.* **39**, 60–69 (2007).
21. Karki, P., Li, X. J., Schrama, D. & Fliegel, L. B-Raf associates with and activates the NHE1 isoform of the Na+/H + exchanger.*J Biol Chem.***286**,13096–13105.
22. Cong, D. *et al.* 2014. Upregulation of NHE1 protein expression enables glioblastoma cells to escape TMZ-mediated toxicity via increased H(+) extrusion, cell migration and survival. *Carcinogenesis*. **35**, 2014–2024. (2011).
23. Bandyopadhyay, S. *et al.* A human MAP kinase interactome. *Nat Methods.* **7**, 801–805 (2010).
24. Meima, M. E., Webb, B. A., Witkowska, H. E. & Barber, D. L. The sodium-hydrogen exchanger NHE1 is an Akt substrate necessary for actin filament reorganization by growth factors. *J Biol Chem.* **284**, 26666–26675 (2009).
25. Wang, H., Cai, J., Du, S. X., Wei, W. & Shen, X. H. LAMC2 modulates the acidity of microenvironments to promote invasion and migration of pancreatic cancer cells via regulating AKT-dependent NHE1 activity. *Exp Cell Res.* **391**, 111984 (2020).
26. Lundquist, J. J. & Dudek, S. M. Differential activation of extracellular signal-regulated kinase 1 and a related complex in neuronal nuclei. *Brain Cell Biol.* **35**, 267–281 (2006).
27. Kolch, W. Coordinating ERK/MAPK signaling through scaffolds and inhibitors. *Nat Rev Mol Cell Biol.* **6**, 827–837 (2005).
28. Wang, X. & Studzinski, G. P. Raf-1 signaling is required for the later stages of 1,25-dihydroxyvitamin D3-induced differentiation of HL60 cells but is not mediated by the MEK/ERK module. *J Cell Physiol.* **209**, 253–260 (2006).
29. Wu, X., Carr, H. S., Dan, I. & Ruvolo, P. P. & Frost J. A. p21 activated kinase 5 activates Raf-1 and targets it to mitochondria. *J Cell Biochem.* **105**, 167–175 (2008).
30. Edmunds, J. W. & Mahadevan, L. C. MAP kinases as structural adaptors and enzymatic activators in transcription complexes. *J Cell Sci.* **117**, 3715–3723 (2004).
31. Ren, J. G., Li, Z. & Sacks, D. B. IQGAP1 modulates activation of B-Raf. *Proc Natl Acad Sci U S A.* **104**, 10465–10469 (2007).
32. Garbe, C., Eigentler, T. K. & Vemurafenib *Recent Results Cancer Res.* **211**, 77–89 (2018).

33. Robinson, G. W., Orr, B. A. & Gajjar, A. Complete clinical regression of a BRAF V600E-mutant pediatric glioblastoma multiforme after BRAF inhibitor therapy. *BMC Cancer.* **14**, 258–262 (2014).
34. Puszkiel, A. *et al.* Clinical Pharmacokinetics and Pharmacodynamics of Dabrafenib. *Clin Pharmacokinet.* **58**, 451–467 (2019).
35. Wang, Y. *et al.* Williams syndrome transcription factor is a target of pro-oncogenic Ser158 phosphorylation mediated by Ras-MAPK pathway in human breast cancer. *Int J Clin Exp Pathol.* **2**, 1668–1675 (2016).

Figures

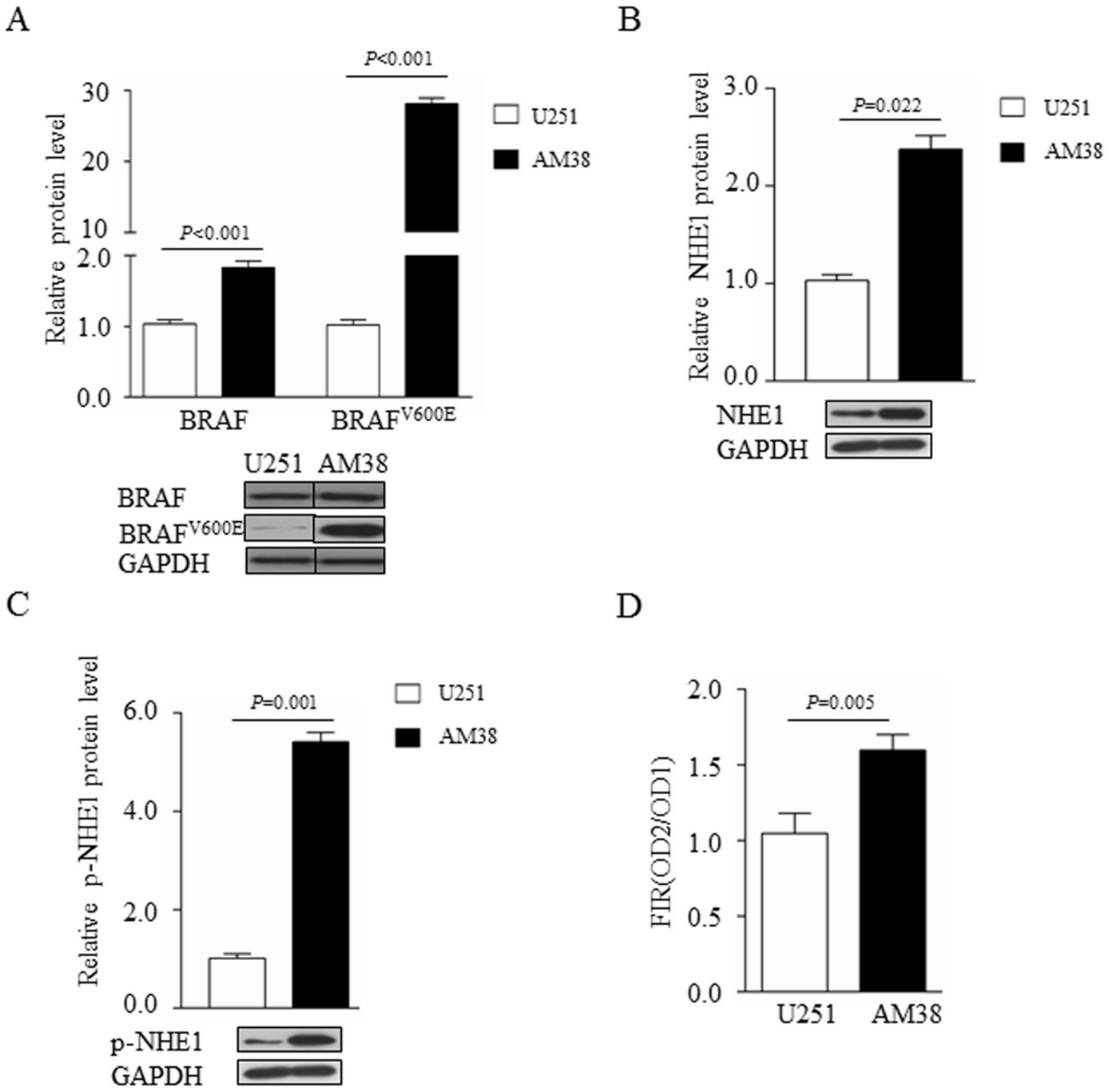

Figure 1

NHE1 was activated in BRAFV600E-mutant AM38 cells (A) The relative proteins levels of BRAF and BRAFV600E in U251 and AM38 cells were analyzed by Western blot with GAPDH as internal control. The relative proteins levels of (B) NHE1 and (C) p-NHE1 in U251 and AM38 cells were analyzed by Western blot with GAPDH as internal control. (D) The NHE1 activity of U251 and AM38 cells were detected by BCECF-AM fluorescent probe. The Fluorescence Intensity Ratio (FIR, FIR=OD2/OD1) at 440 nm and 490 nm was measured by UV-Visible. FIR reflects the pH value and the activity of NHE1 in the cell. The

experiments were repeated three times independently and the results were expressed as mean±standard deviation ($\bar{\chi}$ ±SD).

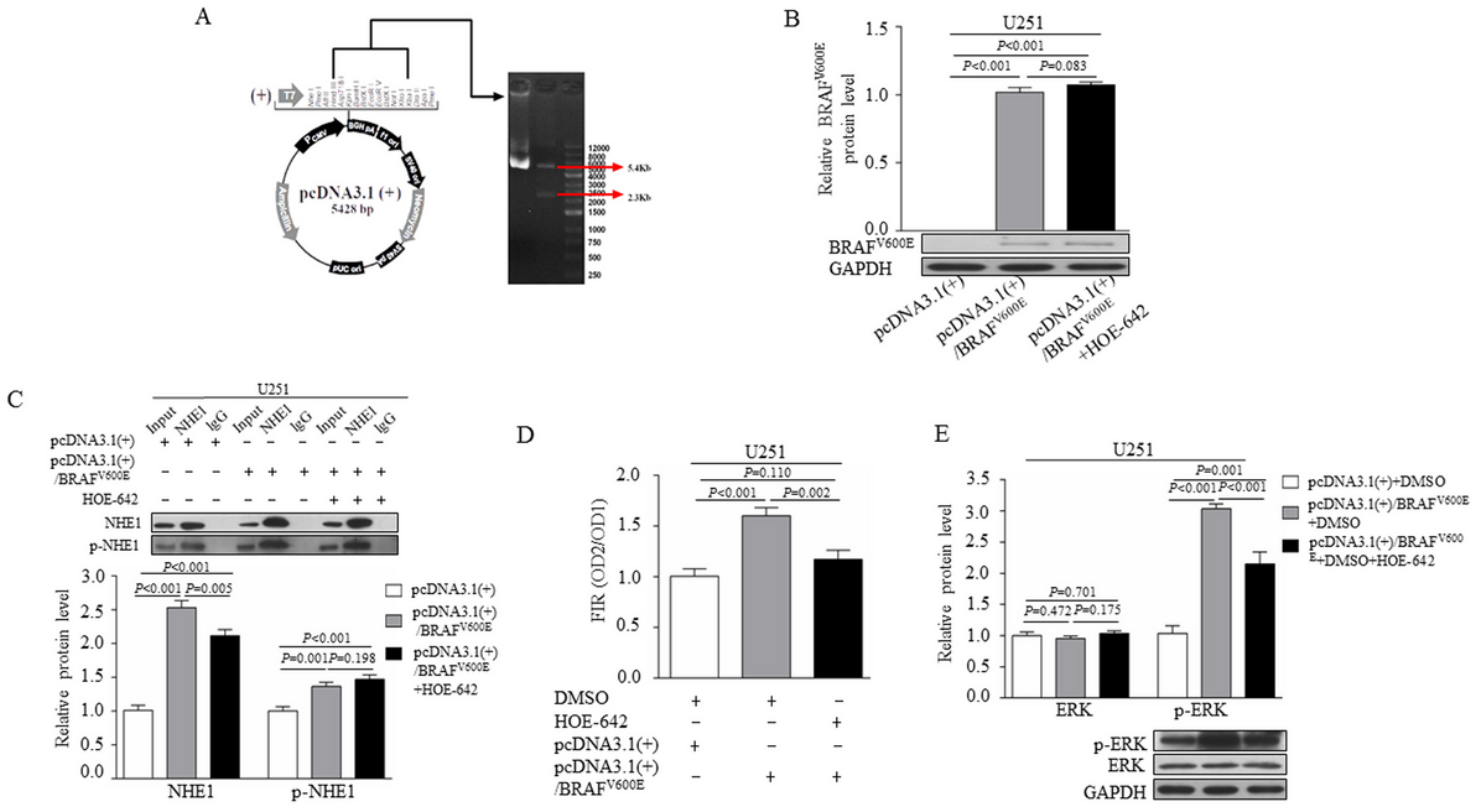

Figure 2

NHE1 was at downstream of BRAFV600E and at upstream of ERK (A) Schematic diagram of the recombinant pcDNA3.1(+)/BRAFV600E plasmids construction. (B) The relative protein levels of BRAFV600E in U251 cells of each group at 48 h post-transfection were verified by Western blot with GAPDH as internal control. (C) The relative protein levels of NHE1 and phosphorylation NHE1 (p-NHE1) in U251 cells of each group were analyzed by Western blot with GAPDH as internal control. (D) The NHE1 activity of U251 cells in each group detected by BCECF-AM fluorescent probe. (E) The relative protein levels of ERK and p-ERK in U251 cells of each group were analyzed by Western blot with GAPDH as internal control. HOE-642 is a NHE1 inhibitor. The experiments were repeated three times independently and the results were expressed as $\bar{\chi}$ ±SD.

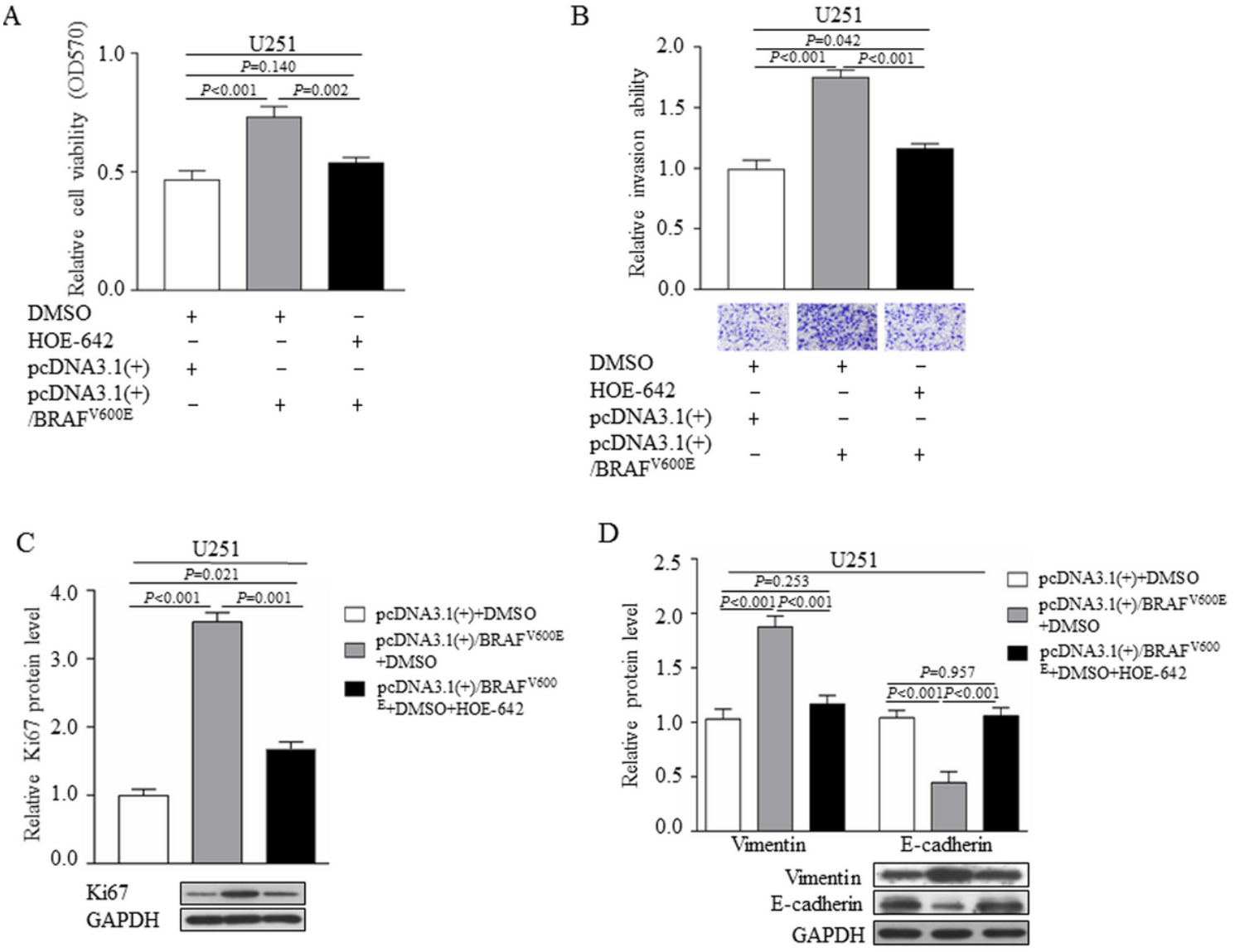

Figure 3

The enhanced expression and invasion abilities of U251 cells induced by BRAFV600E overexpression were inversed by HOE-642 The proliferation (A) and invasion abilities (B) of each group cells at 48 h post-transfection were analyzed by MTT (optical density, OD) and matrigel-transwell assay, respectively. The relative protein levels of Ki67 (C) and Vimentin and E-cadherin (D) in U251 cells of each group were analyzed by Western blot with GAPDH as internal control. HOE-642 is a NHE1 inhibitor. The experiments were repeated three times independently and the results were expressed as $\bar{\chi}$ ±SD.

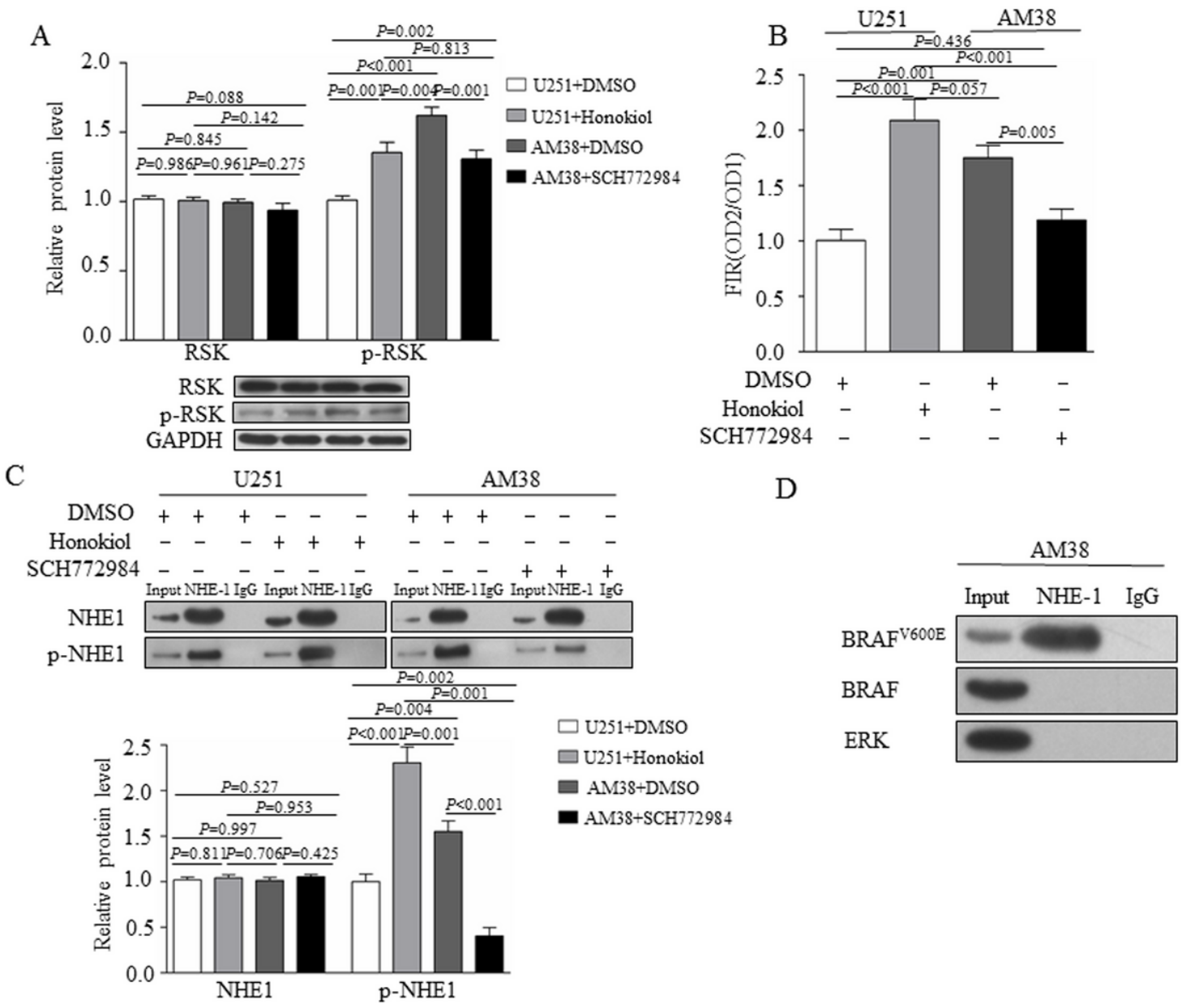

Figure 4

The phosphorylation and activity of NHE1 were positively regulated by ERK activity (A) The relative protein levels of RSK and p-RSK in U251 cells of each group were analyzed by Western blot with GAPDH as internal control. Honokiol is an ERK agonist with anticancer activity, and SCH772984 is a novel specificity ERK inhibitor. (B) The NHE1 activities in U251 and AM38 cells were detected by BCECF-AM fluorescent probe. (C) The NHE1 and p-NHE1 levels in U251 and AM38 cells were analyzed by Western blot with GAPDH as internal control. The experiments were repeated three times independently and the results were expressed as $\bar{\chi}$ ±SD. (D) The interactions of NHE1 between BRAF, BRAFV600E and ERK in AM38 cells were analyzed by immunoprecipitation and Western blot.

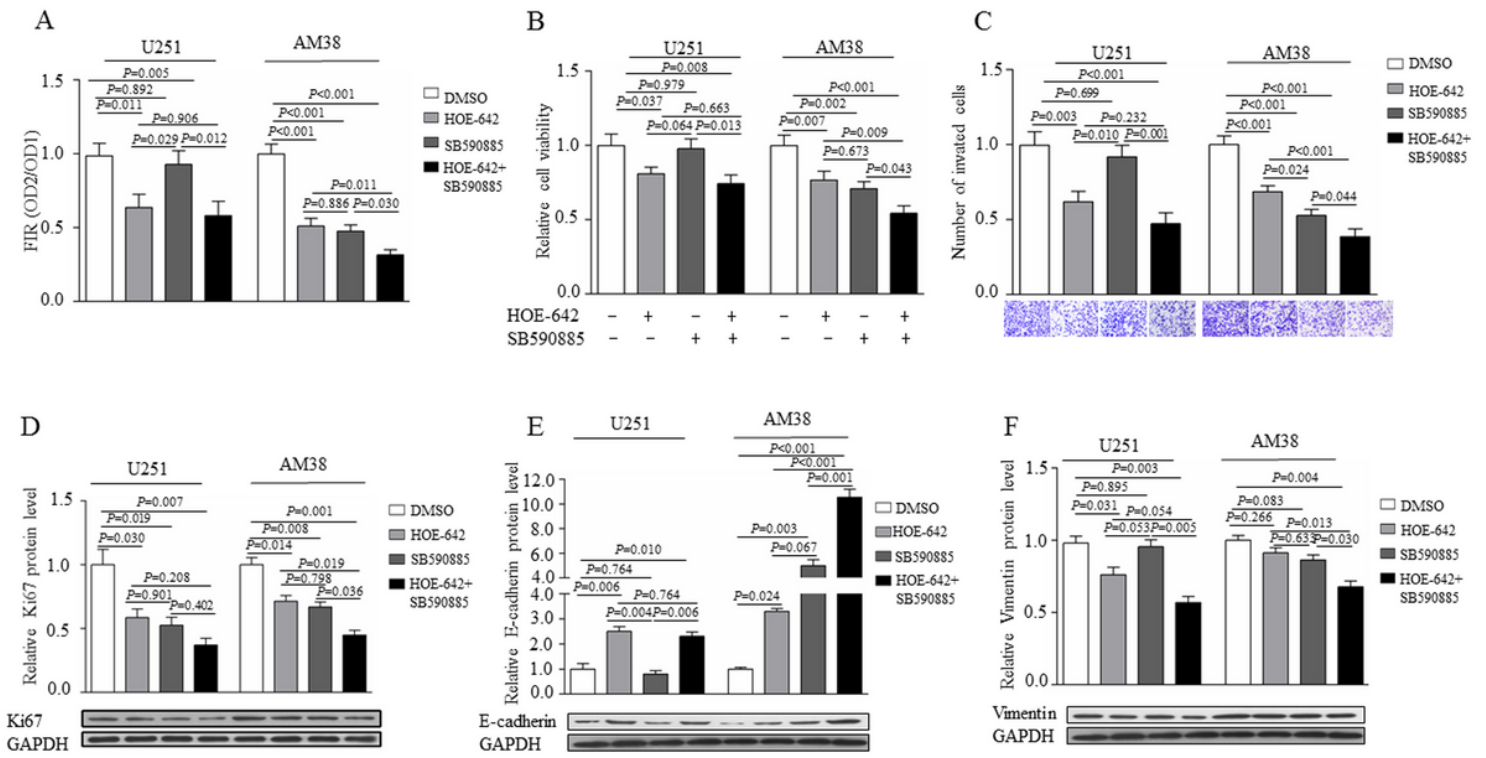

Figure 5

The proliferation and invasion abilities of GBM cells were inhibited by BRAFV600E inhibitor and NHE1 inhibitor alone and combined (A) The NHE1 activity of U251 and AM38 cells were detected by BCECF-AM fluorescent probe. The Fluorescence Intensity Ratio (FIR, FIR=OD2/OD1) at 440 nm and 490 nm was measured by UV-Visible. FIR reflects the pH value and the activity of NHE1 in the cell. HOE-642 is a NHE1 inhibitor, SB590885 is a BRAF inhibitor. (B) The invasion abilities of each group cells at 48 h post-transfection were analyzed by matrigel-transwell assay. The relative protein levels of Ki67 (C) and E-cadherin (D) and Vimentin (E) in U251 cells of each group were analyzed by Western blot with GAPDH as internal control. The experiments were repeated three times independently and the results were expressed as $\bar{\chi}$ ±SD.

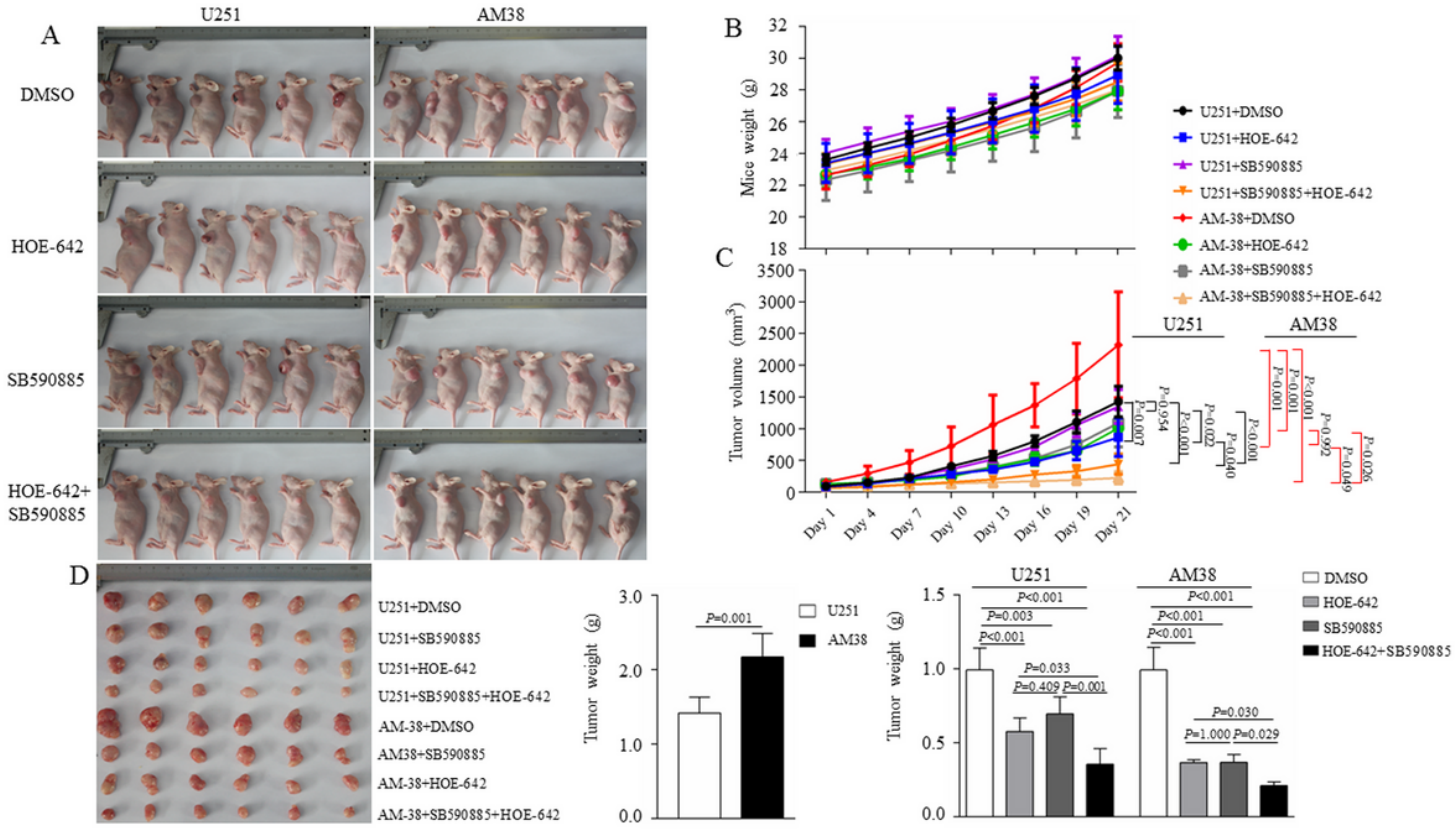

Figure 6

(A) Tumor photos and body photos of nude mice in each group. (B) The nude mouse body weight growth curve and (C) tumor growth curve. The long diameter and short diameter of the tumor were measured and weighed every 3 days, and the growth curve of the transplanted tumor was drawn based on the average tumor volume of each group of animals. (D) Statistics of tumor weight in each group of nude mice. The experiments were repeated three times independently and the results were expressed as $\bar{\chi}$ ±SD.

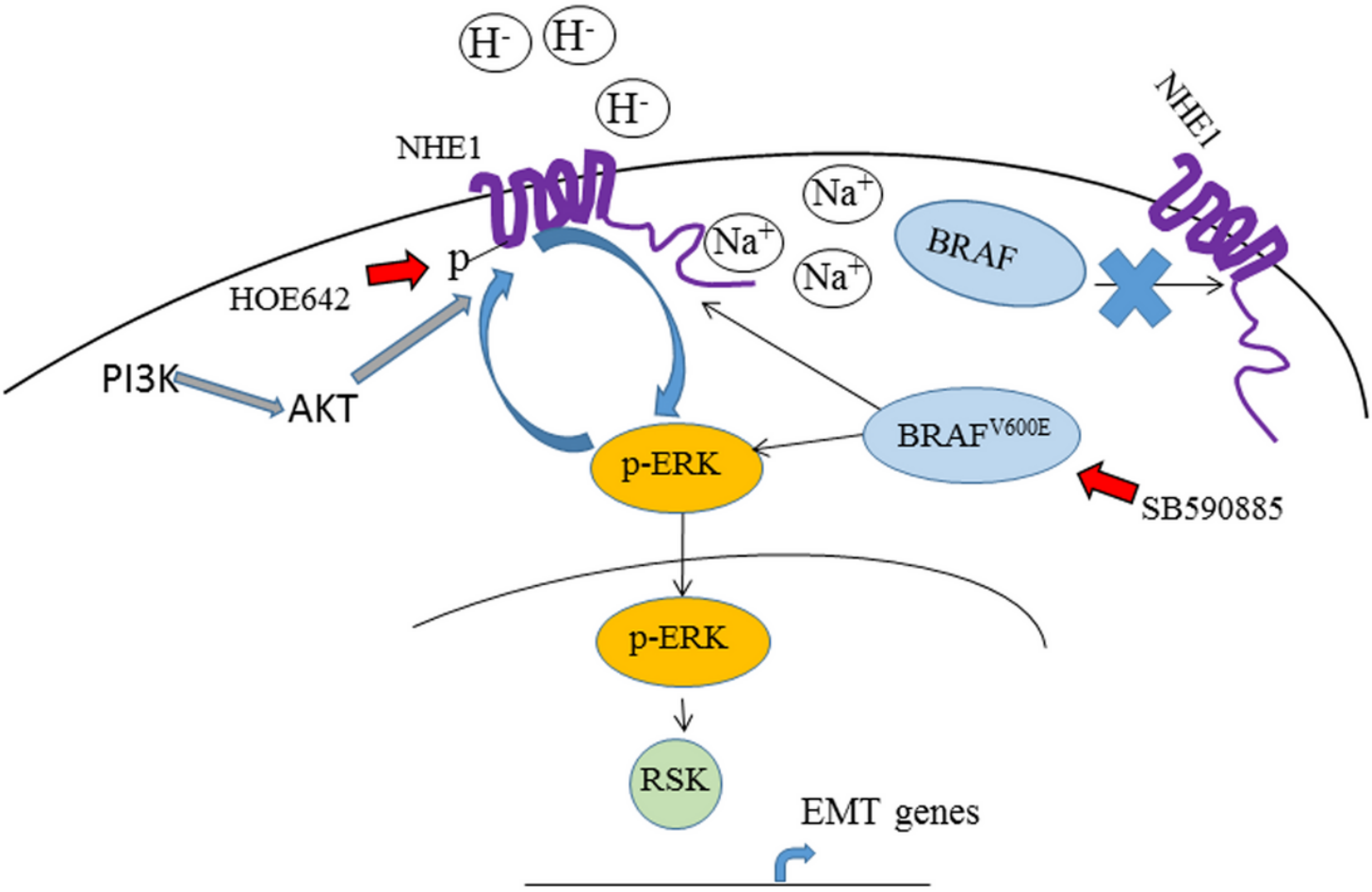

Figure 7

Schematic diagram of the positive feedback between NHE1 and ERK phosphorylation in GBM Cells with BRAFV600E mutation.